rabbits will be useful for studying gene functions relating to atherosclerosis.

9. Conclusion

In humans, clarification of the mechanism of acute coronary syndromes and the development of therapeutics are critical. To accomplish the late Professor Watanabe's goal, we attempted to induce the rupturing of coronary plaques and subsequent formation of thrombi in WHHLMI rabbits. In addition, the development of transgenic WHHLMI rabbits expressing various MMPs or cytokines may help to clarify the mechanisms behind the destabilization of atheromatous plaques, rupturing of plaques, formation of thrombi, and acute coronary syndromes. The WHHL or WHHLMI rabbit will continue contributing to studies of hypercholesterolemia, atherosclerosis, myocardial infarction, and related diseases. Dr. Watanabe's contribution to progress in studies of lipoprotein metabolism and atherosclerosis was substantial and he will be greatly missed.

Acknowledgements

Development of the coronary atherosclerosis-prone WHHL rabbit was supported partly by research grants from the Ministry of Education, Culture, Science and Technology of Japan and a Grant-in-Research on Biological Resources and Animal Models for Drug Development, from the Ministry of Health, Labour and Welfare of Japan. We thank Sankyo Co. Ltd. for their support in the maintenance of the WHHL or WHHLMI rabbit strain from 1980 to 2006.

References

[1] Watanabe Y. Serial inbreeding of rabbits with hereditary hyperlipidemia (WHHL-rabbit). Atherosclerosis 1980;36:261–8.
[2] Goldstein JL, Kita T, Brown MS. Defective lipoprotein receptors and atherosclerosis: lessons from an animal counterpart of familial hypercholesterolemia. N Engl J Med 1983;309:288–96.
[3] Watanabe Y. Studies on characteristics of spontaneously hyperlipemic rabbits and development of the strains with such property. Bull Azabu Vet Coll 1977;2:99–124 (in Japanese).
[4] Watanabe Y, Ito T, Kondo T. Breeding of a rabbit strain of hyperlipidemia and characteristics of the strain. Exp Anim 1977;26:35–42 (in Japanese).
[5] Goldstein JL, Brown MS. Binding and degradation of low density lipoproteins by cultured human fibroblasts, comparison of cells from a normal subject and from a patient with homozygous familial hypercholesterolemia. J Biol Chem 1974;249:5153–62.
[6] Endo A, Kuroda M, Tsujita Y. ML-236A, ML-236B, and ML-236C, new inhibitors of cholesterogenesis produced by Penicillium citrinium. J Antibiot (Tokyo) 1976;29:1346–8.
[7] Tanzawa K, Shimada Y, Kuroda M, Tsujita Y, Arai M, Watanabe Y. WHHL-rabbit: a low density lipoprotein receptor-deficient animal model for familial hypercholesterolemia. FEBS Lett 1980;118:81–4.
[8] Kita T, Brown MS, Watanabe Y, Goldstein JL. Deficiency of low density lipoprotein receptors in liver and adrenal gland of the WHHL rabbit, an animal model of familial hypercholesterolemia. Proc Natl Acad Sci USA 1981;78:2268–72.
[9] Attie AD, Pittman RC, Watanabe Y, Steinberg D. Low density lipoprotein receptor deficiency in cultured hepatocytes of the WHHL rabbit. J Biol Chem 1981;256:9789–92.
[10] Havel RJ, Kita T, Kotite L, et al. Concentration and composition of lipoproteins in blood plasma of the WHHL rabbit. Arteriosclerosis 1982;2:467–74.
[11] Kita T, Goldstein JL, Brown MS, et al. Hepatic uptake of chylomicron remnants in WHHL rabbits: a mechanism genetically distinct from the low density lipoprotein receptor. Proc Natl Acad Sci USA 1982;79:3623–7.
[12] Kita T, Brown MS, Bilheimer DW, Goldstein JL. Delayed clearance of very low density and intermediate density lipoproteins with enhanced conversion to low density lipoprotein in WHHL rabbits. Proc Natl Acad Sci USA 1982;79:5693–7.
[13] Dietschy JM, Kita T, Suckling KE, Goldstein JL, Brown MS. Cholesterol synthesis in vivo and in vitro in the WHHL rabbit, an animal with defective low density lipoprotein receptors. J Lipid Res 1983;24:469–80.
[14] Schneider WJ, Brown MS, Goldstein JL. Kinetic defects in the processing of the low density lipoprotein receptor in fibroblasts from WHHL rabbits and a family with familial hypercholesterolemia. Mol Biol Med 1983;1:353–67.
[15] Yamamoto T, Bishop RW, Brown MS, Goldstein JL, Russell DW. Deletion in cysteine-rich region of LDL receptor impedes transport to cell surface in WHHL rabbit. Science 1986;232:1230–7.
[16] Bilheimer DW, Watanabe Y, Kita T. Impaired receptor-mediated catabolism of low density lipoprotein in the WHHL rabbit, an animal model of familial hypercholesterolemia. Proc Natl Acad Sci USA 1982;79:3305–9.
[17] Pittman RC, Carew TE, Attie AD, et al. Receptor-dependent and receptor-independent degradation of low density lipoprotein in normal rabbits and in receptor-deficient mutant rabbits. J Biol Chem 1982;257:7994–8000.
[18] Hornick CA, Kita T, Hamilton RL, Kane JP, Havel RJ. Secretion of lipoproteins from the liver of normal and Watanabe heritable hyperlipidemic rabbits. Proc Natl Acad Sci USA 1983;80:6096–100.
[19] Son YC, Zilversmit DB. Increased lipid transfer activities in hyperlipidemic rabbit plasma. Arteriosclerosis 1986;6:345–51.
[20] Nakamura M, Taniguchi S, Ishida BY, Kobayashi K, Chan L. Phenotype interaction of apobec-1 and CETP, LDLR, and apoE gene expression in mice, role of apoB mRNA editing in lipoprotein phenotype expression. Arterioscler Thromb Vasc Biol 1998;18:747–55.
[21] Ishibashi S, Goldstein JL, Brown MS, Herz J, Buma DK. Massive xanthomatosis and atherosclerosis in cholesterol-fed low density lipoprotein receptor-negative mice. J Clin Invest 1994;93:1885–93.
[22] Agellon LB, Walsh A, Hayek T, et al. Reduced high density lipoprotein cholesterol in human cholesteryl ester transfer protein transgenic mice. J Biol Chem 1991;266:10796–801.
[23] Kozarsky KF, Bonen DK, Giannoni F, et al. Hepatic expression of the catalytic subunit of the apolipoprotein B mRNA editing enzyme (apobec-1) ameliorates hypercholesterolemia in LDL receptor-deficient rabbits. Hum Gene Ther 1996;7:943–57.
[24] Hilano K, Min J, Funahashi T, Davidson NO. Cloning and characterization of the rat apobec-1 gene: a comparative analysis of gene structure and promoter usage in rat and mouse. J Lipid Res 1997;38:1103–19.
[25] Li X, Catalina F, Grundy SM, Patel S. Method to measure apolipoprotein B-48 and B-100 secretion rates in an individual mouse: evidence for a very rapid turnover of VLDL and preferential removal of B-48 relative to B-100-containing lipoproteins. J Lipid Res 1996;37:210–20.
[26] González-Navarro H, Nong Z, Amar MJ, et al. The ligand-binding function of hepatic lipase modulates the development of atherosclerosis in transgenic mice. J Biol Chem 2004;279:45312–21.
[27] Buja LM, Kita T, Goldstein JL, Watanabe Y, Brown MS. Cellular pathology of progressive atherosclerosis in the WHHL rabbit, an animal model of familial hypercholesterolemia. Arteriosclerosis 1983;3:87–101.
[28] Cybulsky MI, Gimbrone MA. Endothelial expression of a mononuclear leukocyte adhesion molecule during atherogenesis. Science 1991;251:788–91.
[29] Rosenfeld ME, Tsukada T, Gown AM, Ross R. Fatty streak initiation in Watanabe heritable hyperlipidemic and comparably hypercholesterolemic fat-fed rabbits. Arteriosclerosis 1987;7:9–23.
[30] Rosenfeld ME, Tsukada T, Chait A, et al. Fatty streak expansion and maturation in Watanabe heritable hyperlipidemic and comparably hypercholesterolemic fat-fed rabbits. Arteriosclerosis 1987;7:24–34.
[31] Takano T, Amanuma K, Kimura J, Kanaseki T, Ohkuma S. Involvement of macrophages in accumulation and elimination of cholesterol ester in atherosclerotic aorta. Acta Histochem Cytochem 1986;19:135–43.
[32] Tsukada T, Rosenfeld M, Ross R, Gown AM. Immunocytochemical analysis of cellular components in atherosclerotic lesions: use of monoclonal antibodies with the Watanabe and fat-fed rabbit. Arteriosclerosis 1986;6:601–13.
[33] Nakazato K, Ishibashi T, Shindo J, Shiomi M, Maruyama Y. Expression of very low density lipoprotein receptor mRNA in rabbit atherosclerotic lesions. Am J Pathol 1996;149:1831–8.
[34] Hiltunen TP, Luoma JS, Nikkari T, YlaHerttuala S. Expression of LDL receptor, VLDL receptor, LDL receptor-related protein, and scavenger receptor in rabbit atherosclerotic lesions: marked induction of scavenger receptor and VLDL receptor expression during lesion development. Circulation 1998;97:1079–86.
[35] Mowri H, Ohkuma S, Takano T. Monoclonal DLR1a/104G antibody recognizing peroxidized lipoproteins in atherosclerotic lesions. Biochim Biophys Acta 1988;963:208–14.
[36] Boyd HC, Gown AM, Wolfbaur G, Chait A. Direct evidence for a protein recognized by a monoclonal antibody against oxidatively modified LDL in atherosclerotic lesions from a Watanabe heritable hyperlipidemic rabbit. Am J Pathol 1989;135:815–25.
[37] Frank JS, Fogelman AM. Ultrastructure of the intima in WHHL and cholesterol-fed rabbit aortas prepared by ultra-rapid freezing and freeze-etching. J Lipid Res 1989;30:967–8.
[38] Nakajima K, Nakano T, Tanaka A. The oxidative modification hypothesis of atherosclerosis: the comparison of atherogenic effects on oxidized LDL and remnant lipoproteins in plasma. Clin Chim Acta 2006;367:36–47.
[39] Amanuma K, Kanaseki T, Ikeuchi Y, Ohkuma S, Takano T. Studies on fine structure and location of lipids in quick-freeze replicas of atherosclerotic aorta of WHHL rabbits. Virchows Arch A 1986;410:231–8.
[40] Shiomi M, Ito T, Tsukada T, Yata T, Ueda M. Cell composition of coronary and aortic atherosclerotic lesions in WHHL rabbits differ. Arterioscler Thromb 1994;14:931–7.
[41] Shiomi M, Ito T, Tsukada T, et al. Reduction of serum cholesterol levels alters lesional composition of atherosclerotic plaques: effect of pravastatin sodium on atherosclerosis in mature WHHL rabbits. Arterioscler Theromb Vasc Biol 1995;15:1938–2144.
[42] Fukumoto Y, Libby P, Rabkin E, et al. Statins alter smooth muscle cell accumulation and collagen content in established atheroma of Watanabe heritable hyperlipidemic rabbits. Circulation 2001;103:993–9.

[43] Shiomi M, Ito T, Hirouchi Y, Enomoto M. Fibromuscular cap composition is important for the stability of established atherosclerotic plaques in mature WHHL rabbits treated with statins. Atherosclerosis 2001;157:75–84.
[44] Shiomi M, Yamada S, Ito T. Atheroma stabilizing effects of simvastatin due to depression of macrophages or lipid accumulation in the atheromatous plaques of coronary atherosclerosis-prone WHHL rabbits. Atherosclerosis 2005;178:287–94.
[45] Shiomi M, Yamada S, Amano Y, Nishimoto T, Ito T. Lapaquistat acetate (TAK-475), a squalene synthase inhibitor, changes macrophage/lipid-rich coronary plaques of WHHLMI rabbits into fibrous lesions. Br J Pharmacol 2008;154:949–57.
[46] Aikawa M, Rabkin E, Okada Y, et al. Lipid lowering by diet reduces matrix metalloproteinase activity and increases collagen content of rabbit atheromas: a potential mechanism of lesion stabilization. Circulation 1998;97:2433–44.
[47] Watanabe Y, Ito T, Shiomi M. The effect of selective breeding on the development of coronary atherosclerosis in WHHL rabbits, an animal model for familial hypercholesterolemia. Atherosclerosis 1985;56:71–9.
[48] Shiomi M, Ito T, Shiraishi M, Watanabe Y. Inheritability of atherosclerosis and the role of lipoproteins as risk factors in the development of atherosclerosis in WHHL rabbits: risk factors related to coronary atherosclerosis are different from those related to aortic atherosclerosis. Atherosclerosis 1992;96:43–52.
[49] Ito T, Shiomi M. Cerebral atherosclerosis occurs spontaneously in homozygous WHHL rabbits. Atherosclerosis 2001;156:57–66.
[50] Shiomi M, Ito T, Yamada S, Kawashima S, Fan J. Development of an animal model for spontaneous myocardial infarction (WHHLMI rabbit). Arterioscler Thromb Vasc Biol 2003;23:1239–44.
[51] Van der Wall AC, Becker AE, Van der Loos CM, Das PK. Site of intimal rupture or erosion of thrombosed coronary atherosclerotic plaques is characterized by an inflammatory process irrespective of the dominant plaque morphology. Circulation 2001;104:365–72.
[52] Shiomi M, Fan J. Unstable coronary plaques and cardiac events in myocardial infarction-prone Watanabe heritable hyperlipidemic rabbits: questions and quandaries. Curr Opin Lipidol 2008;19:631–6.
[53] Ito T, Yamada S, Shiomi M. Progression of coronary atherosclerosis relates to the onset of myocardial infarction in an animal model of spontaneous myocardial infarction (WHHLMI rabbits). Exp Anim 2004;53:339–46.
[54] Shiomi M, Yamada S, Matsukawa A, Itabe H, Ito T. Invasion of atheromatous plaques into tunica media causes coronary outward remodeling in WHHLMI rabbits. Atherosclerosis 2008;198:287–93.
[55] Liew TV, Ray KK. Intensive statin therapy in acute coronary syndromes. Curr Atheroscler Rep 2008;10:158–63.
[56] Watanabe Y, Ito T, Saeki M, et al. Hypolipidemic effects of CS-500 (ML-236B) in WHHL-rabbit, a heritable animal model for hyperlipidemia. Atherosclerosis 1981;38:27–31.
[57] Tsujita Y, Kuroda M, Shimada Y, et al. CS-514, a competitive inhibitor of 3-hydroxy-3-methylglutaryl coenzyme A reductase: tissue-selective inhibition of sterol synthesis and hypolipidemic effect on various animal species. Biochim Biophys Acta 1986;877:50–60.
[58] Watanabe Y, Ito T, Shiomi M, et al. Preventive effect of pravastatin sodium, a potent inhibitor of 3-hydroxy-3-methylglutaryl coenzyme A reductase, on coronary atherosclerosis and xanthoma in WHHL rabbits. Biochim Biophys Acta 1988;960:294–302.
[59] Kita T, Nagano Y, Yokode M, et al. Probucol prevents the progression of atherosclerosis in Watanabe heritable hyperlipidemic rabbit, an animal model for familial hypercholesterolemia. Proc Natl Acad Sci USA 1987;84:5928–31.
[60] Carew TE, Schwenke DC, Steinberg D. Antiatherogenic effect of probucol unrelated to its hypercholesterolemic effect: evidence that antioxidants in vivo can selectively inhibit low density lipoprotein degradation in macrophage-rich fatty streaks and slow the progression of atherosclerosis in the Watanabe heritable hyperlipidemic rabbits. Proc Natl Acad Sci USA 1987;84:7725–9.
[61] Steen H, Lima JA, Chatterjee S, et al. High-resolution three-dimensional aortic magnetic resonance angiography and quantitative vessel wall characterization of different atherosclerotic stages in a rabbit model. Invest Radiol 2007;42:614–21.
[62] Ogawa M, Ishino S, Mukai T, et al. ^{18}F-FDG accumulation in atherosclerotic plaques: immunohistochemical and PET imaging study. J Nucl Med 2004;45:1245–50.
[63] Iwata A, Miura S, Imaizumi B, Saku K. Measurement of atherosclerotic plaque volume in hyperlipidemic rabbit aorta by intravascular ultrasound. J Cardiol 2007;50:229–34.
[64] Shen J, Herderick E, Cornhill JF, et al. Macrophage-mediated 15-lipoxygenase expression protects against atherosclerosis development. J Clin Invest 1996;98:2201–8.
[65] Brousseau ME, Kauffman RD, Herderick EE, et al. LCAT modulates atherogenic plasma lipoproteins and the extent of atherosclerosis only in the presence of normal LDL receptor in transgenic rabbits. Arterioscler Thromb Vasc Biol 2000;20:450–8.
[66] Fan J, Challah M, Shimoyamada H, et al. Defects of the LDL receptor in WHHL transgenic rabbits lead to a marked accumulation of plasma lipoprotein(a). J Lipid Res 2000;41:1004–12.
[67] Koike T, Liang J, Wang X, et al. Overexpression of lipoprotein lipase in transgenic Watanabe heritable hyperlipidemic rabbits improves hyperlipidemia and obesity. J Biol Chem 2004;279:7521–9.
[68] Sun H, Koike T, Ichikawa T, et al. C-reactive protein in atherosclerotic lesions: its origin and pathophysiological significance. Am J Pathol 2005;167:1139–48.
[69] Fan J, Watanabe T. Transgenic rabbits as therapeutic protein bioreactors and human disease models. Pharmacol Ther 2003;99:261–82.

特集

ここまできた神経画像

PETと静脈内投与型O-15標識O_2剤による脳酸素代謝率の測定

天滿　敬
TEMMA Takashi
京都大学大学院薬学研究科病態機能分析学分野

脳循環疾患の病態は酸素代謝率などの脳循環代謝パラメータ変化と密接に関連し，同パラメータ測定の臨床上の有用性が認められているが，小動物での測定法の欠如が，病態解明・治療法開発を目的とした基礎研究の妨げとなっていた．そこで，人工肺を用いて静脈内投与型O-15標識O_2剤の開発をおこない，PET法によるラット脳局所酸素代謝率測定を可能とするとともに，慢性高血圧が脳卒中発症後急性期の機能障害進行を増悪する可能性を見出した．

Key Words
脳酸素代謝率，脳循環疾患，小動物，PET，静脈内投与型O-15標識O_2剤

はじめに

脳梗塞などの脳循環疾患において，その病態は，脳血流量（Cerebral Blood Flow：CBF），脳酸素摂取率（Oxygen Extraction Fraction：OEF），脳酸素代謝率（Cerebral Metabolic Rate for Oxygen：$CMRO_2$）などの脳循環代謝パラメータの変化と密接に関連している．そのため，半減期2分のポジトロン放出核種であるO-15で標識された酸素ガス（^{15}O-O_2ガス）を用いたポジトロン断層撮像法（Positron Emission Tomography：PET）によるOEF，$CMRO_2$の定量測定法が開発され，脳循環疾患の診断，治療方針の決定，予後予測などにおいて，その臨床上の有用性が高く評価されている[1)~3)]．しかし，^{15}O-O_2産生のためのサイクロトロン・ビーム系統の実施準備に時間を要すること，測定に数十分を要すること，治療の緊急性などの観点から，臨床において本法を脳循環疾患発症後超急性期に適用することは難しく，発症後超急性期における脳循環代謝状態の変化についてはほとんど検討されていない．

脳循環疾患発症後超急性期における脳循環代謝状態を検討するためには，動物を用いた基礎検討の必要性が認識されているが，ラットなどの小動物への^{15}O-O_2ガス吸入法の適用は手技上困難であり，PETによる小動物でのOEF，$CMRO_2$の局所定量測定はこれまでおこなわれていなかった．そこでわれわれは，静脈内投与型O-15標識O_2剤（injectable ^{15}O-O_2）の開発，および，それを用いた小動物でのOEF，$CMRO_2$定量測定をおこない，脳卒中発症後超急性期の脳循環代謝機能障害を明らかとする検討をおこなってきたので以下に紹介する．

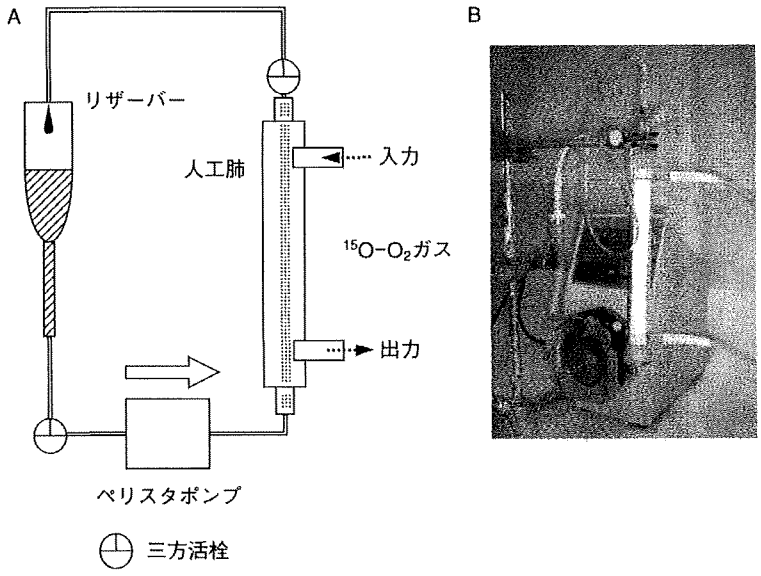

図❶ Injectable ^{15}O-O_2調製システム
A：模式図，B：写真

1 静脈内投与型 O-15 標識 O_2剤 (injectable ^{15}O-O_2) の開発

^{15}O-O_2ガス吸入法に代わり，小動物における高精度 OEF，$CMRO_2$測定を可能とするため，静脈内投与型 O-15 標識 O_2剤 (injectable ^{15}O-O_2) の開発を計画した[4]．^{15}O-O_2ガスの生体への静脈内投与を可能にするには，①^{15}O-O_2ガスを静脈内投与可能な担体に安定的に溶解できること，②担体の酸素結合能が生体内ヘモグロビンと同等であること，③担体の生体適合性が高く毒性が低いこと，④担体の体内動態が血液と同等であること，⑤^{15}O-O_2ガス取り込み率が高く PET 撮像に十分な放射能を有すること，を満たす必要がある．そこで本研究では，①～④の条件，および OEF，$CMRO_2$を正確に評価できる可能性を重視し，injectable ^{15}O-O_2の担体には血液そのものを用いることとした．また，⑤を満たすため，効率的なガス交換の実現が可能と期待される人工肺に着目した．

人工肺は，ポリプロピレン中空糸内部還流型のラット用小型人工肺を作製した．作製した人工肺は，インフュージョンラインキットのリザーバー部と，シリコンチューブを用いて閉鎖系に繋ぎ，蠕動ポンプをシリコンチューブにセットした．ラットより採取した血液を回路内に添加し，さらに，サイクロトロンから供給される^{15}O-O_2ガスの導入・排出ラインを人工肺に接続することで，血液循環型の閉鎖系回路として injectable ^{15}O-O_2標識システムを構築した（図❶）．このシステムの開発により，PET による小動物での酸素代謝の局所定量測定が可能となった[4]．

2 Injectable ^{15}O-O_2-PET 法による正常ラットでの脳酸素代謝率の評価

^{15}O-O_2ガス吸入法では，吸入された^{15}O-O_2は肺でのガス交換機構により血液中に取り込まれ体内を循環する．開発した injectable ^{15}O-O_2は直接静脈内へ^{15}O-O_2を投与するものであるが，PET で取得しうる生体内での放射能循環挙動は両手法とも血液中に取り込まれた^{15}O-O_2に由来することから，injectable ^{15}O-O_2を用いた OEF，$CMRO_2$の解析には^{15}O-O_2ガス単回吸入法における解析手法を応用可能と考えた（図❷）．すなわち CBF，OEF，$CMRO_2$はそれぞれ図❸ (1)-(3) 式から算出される[2)5)]．

実験は，まず CBF 定量測定のため，ペントバルビタール麻酔下，^{15}O-H_2O を正常ラットに静脈内投与し PET 撮像・大腿動脈採血をおこない，ついで体内残存放射能の減衰を約 20 分待った後，injectable ^{15}O-O_2を投与して PET 撮像・大腿動脈採血をおこなった．採血した血液は遠心分離後に血球・血漿中放射能を測定すること

で，^{15}O-O_2画分・^{15}O-H_2O 画分に分けて入力関数を得た[4]．

得られたラット脳の PET 画像上に関心領域（Region of interest：ROI）を設定し CBF，OEF，$CMRO_2$を算出した．その結果（表❶），OEF は，PET 撮像後速やかに大腿動脈および上矢状静脈洞より採血し動静脈酸素分圧較差から直接求めた値（Surgical OEF）と一致し，また，その OEF より算出した $CMRO_2$は外科的な直接測定法により測定した既報[6]と一致した．

これまでおこなわれていた動静脈酸素分圧較差による OEF 算出法は全脳 OEF のみを評価対象とし，また，侵襲的であることから，同一個体におけるくり返し測定は困難であるが，injectable ^{15}O-O_2-PET 法はくり返し小動物における OEF，$CMRO_2$の局所定量測定を可能とするものである．

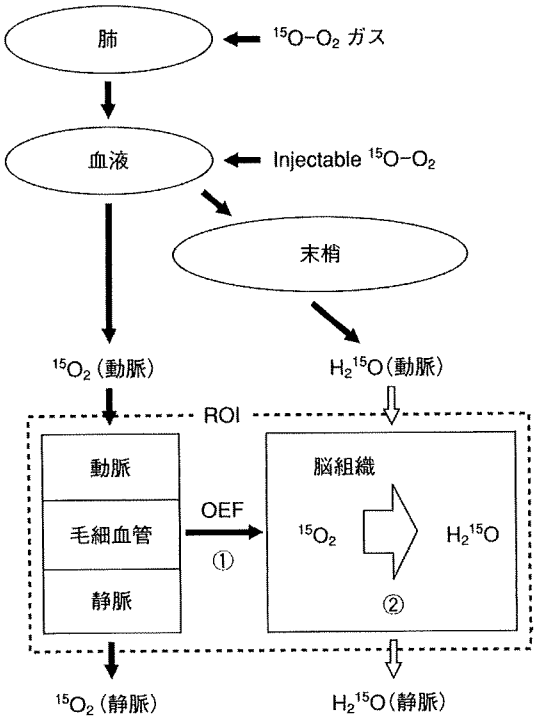

図❷ Injectable ^{15}O-O_2の体内動態模式図
^{15}O-O_2ガス吸入法，injectable ^{15}O-O_2法のいずれにおいても，PET 解析対象となる放射能循環挙動は血液中に取りこまれた^{15}O-O_2に由来することから，injectable ^{15}O-O_2の解析には^{15}O-O_2ガス単回吸入法の方法論を利用可能であると考えられる．
①体内へ投与された^{15}O-O_2は脳毛細血管において酸素摂取率（OEF）に従い脳組織中へ移行する
②脳組織中へ移行した^{15}O-O_2は速やかに^{15}O-H_2O に代謝される

3 脳循環疾患モデルラットでの脳酸素代謝率の評価

脳卒中発症後の脳循環代謝パラメータ変化に関する検討は，これまでにいくつかのモデル動物を用いておこなわれてきている．大型モデル動物では，脳卒中発症後における^{15}O-H_2O や^{15}O-O_2ガスを用いた PET 測定により，脳卒中発症早期に CBF 低下と代償性 OEF 上昇を示す部位は梗塞に陥りにくく，OEF は脳梗塞進展の予測因子となりえることが示されてきている．一方，ラットを用いた基礎研究においても脳卒中発症早期の CBF が梗塞の予測因子となりえることが示されてきているが，CBF は直接エネルギー代謝を反映しないことから，正確な脳組織生存能を評価するためには OEF や $CMRO_2$の測定が必須である．そこで，われわれが開発した injectable ^{15}O-O_2-PET 法を用いて，脳循環疾患モデルラット〔栓子法による右中大脳動脈永久閉塞（middle cerebral

$$(1)\ R(t)=CBF\cdot A_W(t)\otimes e^{-\left(\frac{CBF}{p}+\lambda\right)\cdot t}$$

$$(2)\ R(t)=OEF\cdot CBF\cdot A_O(t)\otimes e^{-\left(\frac{CBF}{p}+\lambda\right)\cdot t}+CBF\cdot A_W(t)\otimes e^{-\left(\frac{CBF}{p}+\lambda\right)\cdot t}+V_B\cdot R\cdot(1-V'_V\cdot OEF)\cdot A_O(t)$$

$$(3)\ CMRO_2=\frac{1.39\cdot Hb\cdot \%Sat}{100}\cdot OEF\cdot CBF$$

図❸ Injectable ^{15}O-O_2の解析式
CBF：脳血流量，OEF：酸素摂取率，$CMRO_2$：脳酸素代謝率
R(t)：脳組織中 O-15 放射能濃度，$A_W(t)$：動脈血中^{15}O-H_2O 放射能濃度，$A_O(t)$：動脈血中^{15}O-O_2放射能濃度
p：水の脳血液分配係数（0.8），λ：O-15 の物理的壊変定数
V_B：脳血液量（0.04 mL/g），R：中枢末梢ヘマトクリット比（0.85），V'_V：脳内有効静脈率（0.835）
Hb：血中ヘモグロビン濃度（g/mL），%Sat：血中酸素飽和パーセント，⊗：重量積分

artery occlusion：MCAO）ラット〕での脳酸素代謝機能を測定した[7]．

その結果（図❹），障害側である右脳は，閉塞1時間後においてCBF減少と代償的なOEF上昇を示したが，24時間後では著しいCBF減少とともにOEFの代償的上昇は消失していた．$CMRO_2$は，非障害側である左脳において1時間後，24時間後で変化しなかった．一方，右脳の$CMRO_2$は左脳とくらべて有意に小さく，さらに，24時間後では1時間後とくらべて有意に低下していた．なお正常側$CMRO_2$は，閉塞1時間後，24時間後とも，外科的手法により求めたラット正常脳の値[8]と同等であった．

臨床において，慢性的な脳循環障害によって脳還流圧が低下しCBFが減少すると，$CMRO_2$を維持するため代償的にOEFが上昇するが，還流圧低下が顕著になると代償性OEF上昇機構は破綻し著しい$CMRO_2$減少に至ることが知られている．上記の結果は，急性モデルではあるが，ラットにおいても酸素代謝に関する代償機構が存在し機能することをはじめて示したものである．

4 脳卒中発症後超急性期の脳循環代謝機能に与える高血圧の影響について

高血圧は疫学的に脳卒中と関連が強く，脳卒中罹患率・死亡率との間には正の相関がある．最近では，高血圧は脳卒中発症後の治療成績にも影響を及ぼし，高血圧を有する脳卒中患者では予後が悪いことが報告されてきている[9]．

慢性高血圧は，脳血管や周囲組織に長期にわたり負荷を与えることから，CBF，OEF，$CMRO_2$の障害応答性を変化しうる[10]．しかしながら，これらの脳循環代謝パラメータを脳卒中発症後超急性期の患者で評価することは，

表❶ 正常ラット脳循環代謝パラメータ
（Magata Y *et al*, 2003[4]より引用）

	Injectable ^{15}O-O_2-PET	Surgical
CBF（mL/min/g）	44±4.5	—
OEF	0.54±0.11	0.57±0.13
$CMRO_2$（mL/min/100 g）	4.3±1.3	—

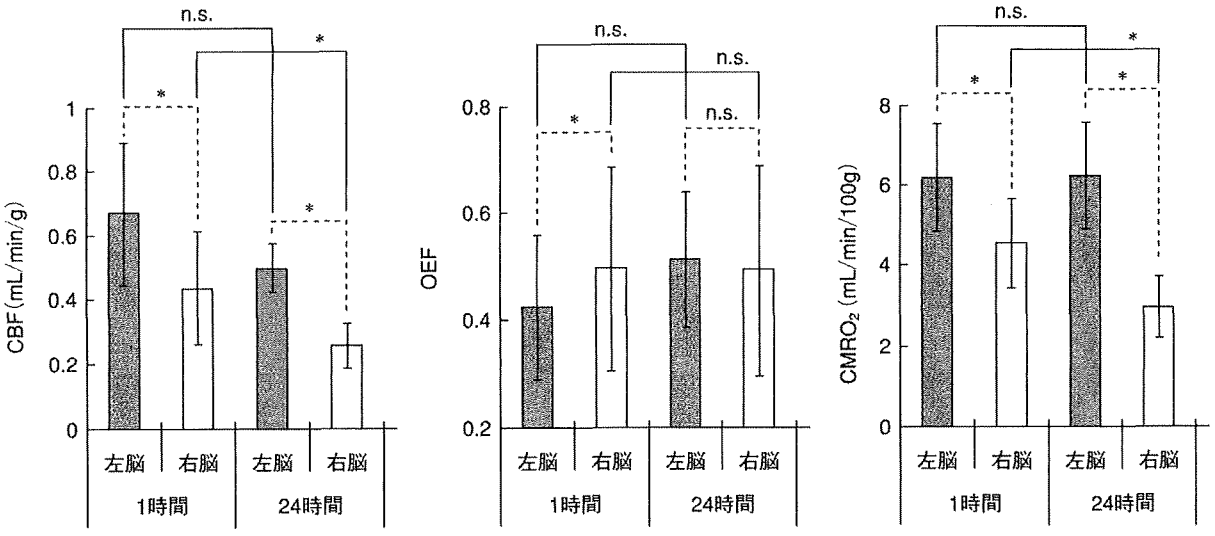

図❹ MCAO処置ラット（閉塞1時間，24時間）の左右脳での脳循環代謝パラメータ
（Temma T *et al*, 2006[7]より引用）
MCAO障害側は右脳
有意差検定は，Wilcoxon signed rank test（左脳 vs 右脳），Mann-Whitney U test（1時間 vs 24時間）によりおこなった．
*$P<0.05$, n.s. not significant.

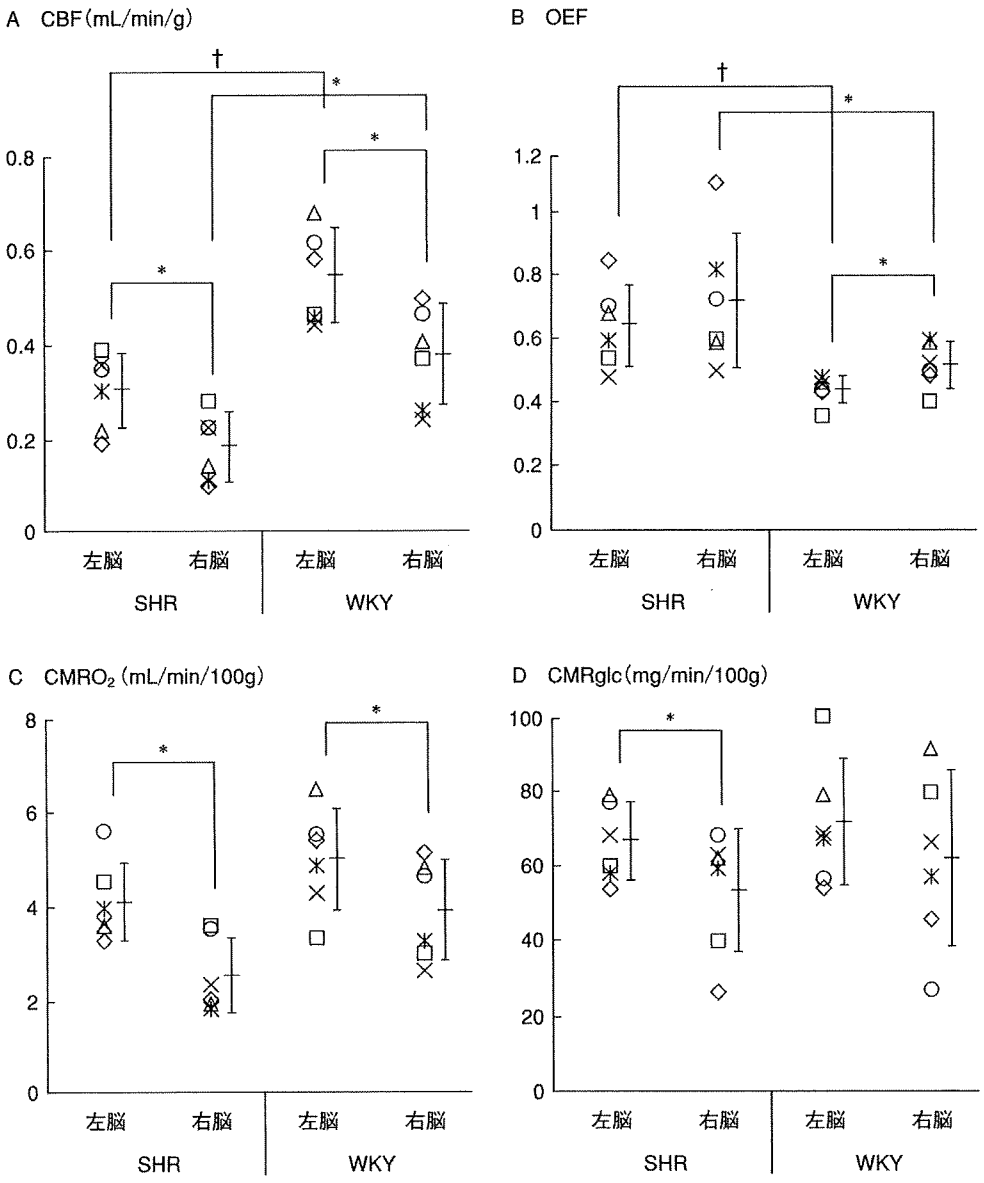

図❺ MCAO（閉塞 1 時間）処置 SHR・WKY ラットの左右脳での脳循環代謝パラメータ
(Temma T *et al*, 2008[13]より引用)
MCAO 障害側は右脳
有意差検定は，Wilcoxon signed rank test（左脳 vs 右脳），Mann-Whitney U test (SHR vs WKY) によりおこなった．
*P＜0.05，†P＜0.01

治療可能時間域（発症後 3 時間）の制限のため現実的でない．これまでに，高血圧モデル動物として自然発症高血圧ラット（Spontaneously Hypertensive Rat：SHR）を用いた検討がなされているが，手技的な限界により CBF と脳梗塞体積のみが評価されているだけで[11)12)]，高血圧が脳卒中発症後急性期の脳循環代謝機能障害に及ぼす影響についてはいまだ明らかではない．そこで，脳卒中発症後超急性期の脳循環代謝パラメータ変化に与える高血圧の影響を明らかにすることを目的として，SHR に 1 時間の右 MCAO を処置し^{15}O-H_2O，injectable ^{15}O-O_2を用いて CBF，OEF，$CMRO_2$の定量測定をおこなった[13)]．

その結果（図❺），SHR では対照の Wistar Kyoto ラット（WKY）とくらべ，両側 CBF の低下[14)]と両側 OEF の上昇が認められたが，$CMRO_2$では明らかな系統差は消失していたことから，SHR では代謝性の代償機構が有効に機能

していることが示された．しかしながら，SHR 右脳では WKY 右脳とくらべて $CMRO_2$低下傾向が認められ，OEF が個体により大きくばらついたことから，SHR 右脳の代償機構は不完全であり，WKY とくらべて虚血障害の進行が速やかであることが示唆された．さらに，エネルギー代謝機能を詳細に調べるため，2-^{18}F-fluoro-2-deoxy-D-glucose（^{18}F-FDG）を用いた脳グルコース代謝率（Cerebral Metabolic Rate for Glucose：CMRglc）定量測定をあわせて実施したところ，SHR においてのみ左右差が認められた．これは，WKY 障害側では虚血コア周辺領域における嫌気的解糖系の亢進を起因とする^{18}F-FDG の集積増加が起こり[14]，半球ベースの解析では左右差が生じなかったためと考えられる．また，MCAO7 時間後に梗塞面積を調べたところ SHR において WKY と比較して有意に広い結果となった．

以上，injectable ^{15}O-O_2-PET 法を MCAO 処置 SHR に適用することで，慢性的な高血圧が脳卒中の発症だけでなく発症後の脳虚血障害の進行にも影響を及ぼすことを見出した．この結果は，基礎疾患の有無（程度）によって脳卒中発症後の虚血障害進行が発症ごく早期から異なることを形態変化が現れる以前に酸素代謝の観点からはじめて明らかにしたものである．今後，これを発展させることで，t-PA が真に効果的な発症後時間域のテーラーメイド評価など，臨床ではきわめて困難な研究を，ラットを用いた injectable ^{15}O-O_2-PET 法により推進できる可能性を有するものと期待される．

おわりに

今回開発した静脈内投与可能な O-15 標識 O_2剤を用いる injectable ^{15}O-O_2-PET 法は，従来不可能であった小動物での OEF，$CMRO_2$の非侵襲的局所定量測定を可能にし，高血圧が脳卒中発症後急性期の脳循環代謝機能障害に関与することを明らかにした．これらの知見は，今後の脳循環疾患の病態解明および診断・治療法開発に有益な情報を提供するものと考えられる．

●文　献●

1) Grubb RL Jr *et al*：Importance of hemodynamic factors in the prognosis of symptomatic carotid occlusion. *JAMA* **280**：1055-1060, 1998

2) Mintun MA *et al*：Brain oxygen utilization measured with O-15 radiotracers and positron emission tomography. *J Nucl Med* **25**：177-187, 1984

3) Yamauchi H *et al*：Uncoupling of oxygen and glucose metabolism in persistent crossed cerebellar diaschisis. *Stroke* **30**：1424-1428, 1999

4) Magata Y *et al*：Development of injectable O-15 oxygen and estimation of rat OEF. *J Cereb Blood Flow Metab* **23**：671-676, 2003

5) Shidahara M *et al*：Evaluation of a commercial PET tomograph-based system for the quantitative assessment of rCBF, rOEF and $rCMRO_2$ by using sequential administration of ^{15}O-labeled compounds. *Ann Nucl Med* **16**：317-327, 2002

6) Sinha AK *et al*：Effect of pentobarbital on cerebral regional venous O_2 saturation heterogeneity. *Brain Res* **591**：146-150, 1992

7) Temma T *et al*：Estimation of oxygen metabolism in a rat model of permanent ischemia using positron emission tomography with injectable ^{15}O-O_2. *J Cereb Blood Flow Metab* **26**：1577-1583, 2006

8) Koźniewska E *et al*：V2-like receptors mediate cerebral blood flow increase following vasopressin administration in rats. *J Cardiovasc Pharmacol* **15**：579-585, 1990

9) Sprigg N *et al*：Relationship between outcome and baseline blood pressure and other haemodynamic measures in acute ischaemic stroke：data from the TAIST trial. *J Hypertens* **24**：1413-1417, 2006

10) Fujishima M *et al*：Autoregulation of cerebral blood flow in young and aged spontaneously hypertensive rats (SHR). *Gerontology* **30**：30-36, 1984

11) Jacewicz M *et al*：The CBF threshold and dynamics for focal cerebral infarction in spontaneously hypertensive rats. *J Cereb Blood Flow Metab* **12**：359-370, 1992

12) Dogan A *et al*：Intraluminal suture occlusion of the middle cerebral artery in spontaneously hypertensive rats. *Neurol Res* **20**：265-270, 1998

13) Temma T *et al*：PET O-15 cerebral blood flow and metabolism after acute stroke in spontaneously hypertensive rats. *Brain Res* **1212**：18-24, 2008

14) Kita H *et al*：Cerebral blood flow and glucose metabolism of the ischemic rim in spontaneously hypertensive stroke-prone rats with occlusion of the middle cerebral artery. *J Cereb Blood Flow Metab* **15**：235-241, 1995

てんま・たかし

天滿　敬　京都大学大学院薬学研究科病態機能分析学分野

1977 年，滋賀県生まれ．
2000 年，京都大学薬学部薬学科卒業．2002 年，京都大学大学院薬学研究科医療薬科学専攻修士課程修了．2004 年，京都大学大学院薬学研究科医療薬科学専攻博士後期過程中退，京都大学大学院薬学研究科助手．2007 年，同助教．2008 年，京都大学博士（薬学）．専門は，放射性医薬品学，分子イメージング学．研究テーマは，脳卒中・がん・動脈硬化を標的とした分子プローブ開発と分子イメージング法にもとづく病態解析．趣味は音楽活動（吹奏楽，ピアノ，歌，ドラム）と水泳．

Eur J Nucl Med Mol Imaging (2010) 37:468–482
DOI 10.1007/s00259-009-1284-9

ORIGINAL ARTICLE

FDG PET as a prognostic predictor in the early post-therapeutic evaluation for unresectable hepatocellular carcinoma

Tatsuya Higashi · Etsuro Hatano · Iwao Ikai · Ryuichi Nishii · Yuji Nakamoto · Koichi Ishizu · Tsuyoshi Suga · Hidekazu Kawashima · Kaori Togashi · Satoru Seo · Koji Kitamura · Yasuji Takada · Shinji Kamimoto

Received: 11 June 2009 / Accepted: 4 September 2009 / Published online: 17 October 2009

Abstract
Purpose To elucidate the prognostic role of post-therapeutic ^{18}F-fluorodeoxyglucose (^{18}F-FDG) positron emission tomography (PET), we conducted a retrospective cohort study analysing the clinical factors that affect overall survival after non-operative therapy for unresectable hepatocellular carcinoma (HCC).
Methods Sixty-seven cases with unresectable HCC who received non-operative therapy (transcatheter arterial chemoembolization: n=24, transcatheter arterial infusion chemotherapy: n=31, radiofrequency ablation: n=5 or systemic chemotherapy: n=7) and had received FDG PET for the evaluation of the therapeutic effect within 1 month after the end of the therapy were evaluated. Overall survival rate was evaluated using the univariate and multivariate analyses of relevant clinical and laboratory parameters before and after therapy, including visual PET analysis and quantitative analysis using maximum standardized uptake value (SUV).
Results Visual PET diagnosis of post-therapeutic lesions was a good predictor of overall survival of unresectable HCC patients. The low FDG group showed significantly longer survival (average: 608 days) than that (average: 328 days) of the high FDG group (p<0.0001). Multivariate analysis showed four significant prognostic factors for the survival: post-therapeutic alpha-fetoprotein (αFP) level (=400 ng/ml, p=0.004), post-therapeutic visual PET diagnosis (p=0.006), post-therapeutic clinical stage (UICC stage IV, p=0.04) and post-therapeutic Milan criteria (p=0.03), while pre-therapeutic clinical factors, SUV by post-therapeutic FDG PET (5.0 or more) or others did not show significance.
Conclusion The present study suggests that post-therapeutic PET performed within 1 month after non-operative therapy can be a good predictor of overall survival in unresectable HCC patients, while pre-therapeutic evaluation including PET, tumour markers and clinical staging may not be useful.

Keyword FDG · Hepatocellular carcinoma · PET · Early prediction · Prognosis · Response · Non-operative therapy

T. Higashi (✉) · R. Nishii
Shiga Medical Center Research Institute,
5-4-30, Moriyama,
Moriyama City, Shiga 524-8524, Japan
e-mail: higashi@shigamed.jp

E. Hatano · I. Ikai · S. Seo · K. Kitamura · Y. Takada · S. Kamimoto
Department of Gastroenterological Surgery,
Kyoto University Graduate School of Medicine,
54 Kawahara-cho, Shogoin,
Sakyo-ku, Kyoto 606-8507, Japan

Y. Nakamoto · K. Ishizu · T. Suga · H. Kawashima · K. Togashi
Department of Diagnostic Imaging and Nuclear Medicine,
Kyoto University Graduate School of Medicine,
54 Kawahara-cho, Shogoin,
Sakyo-ku, Kyoto 606-8507, Japan

Introduction

Hepatocellular carcinoma (HCC) is one of the most frequently occurring tumours worldwide and ranks fifth in frequency in the world [1, 2]. Resection and transplantation achieve the best outcomes in well-selected candidates; however, the 5-year survival rate is only 60–70% [3, 4].

Therefore, a large proportion of patients with HCC were treated with non-operative therapy, because of high risk factors, such as non-localized multiple intrahepatic lesions, extensive vascular invasion or extrahepatic metastasis or because of the shortage of donor livers for transplantation. At the present time, transcatheter arterial chemoembolization (TACE) and transcatheter arterial infusion chemotherapy (TAI) are the main non-operative therapies for relatively large or advanced intrahepatic HCC, while radiofrequency ablation (RFA) and percutaneous ethanol injection therapy (PEIT) are the main non-operative therapies for relatively small HCCs which present in small quantities [5]. For patients with distant metastasis, systemic chemotherapy is supposed to be the best choice. Recently, sorafenib, a multi-targeted tyrosine kinase inhibitor, was found to improve survival of patients with advanced stage HCC [6]. The clinical role of non-operative therapies will become more important in the near future.

In general, the therapeutic response of HCC to non-operative therapy is assessed by conventional radiological imaging modalities, based on the Response Evaluation Criteria in Solid Tumors [7]. However, such criteria using conventional imaging modalities have shown their limitations because therapeutic response and tumour viability are not appropriately reflected in patients with HCC [8]. It was reported in post-operative HCC patients that intrahepatic recurrence could be predicted by several factors, such as the presence of microvascular invasion, poor histological differentiation and satellite lesions [9, 10]. However, these factors based on pathological evaluation cannot be utilized for the evaluation of patients with unresectable HCC treated with non-operative therapy. There is really a call for an appropriate indicator of tumour viability and a predictor of prognosis in patients after non-operative therapy, especially one using a non-invasive imaging modality.

The uptake of ^{18}F fluorodeoxyglucose (^{18}F-FDG), based on the enhanced glucose metabolism in cancer cells, is supposed to be a sensitive marker of tumour viability. Tumour detection using increased ^{18}F-FDG uptake by positron emission tomography (PET) has therefore been applied in diagnostic imaging for a variety of tumours, including HCC [11, 12]. Several studies in liver tumours have shown that FDG PET is useful for tumour characterization, assessment of therapeutic response and outcome [13–15]. On the other hand, other reports showed that the sensitivity of FDG PET is not sufficiently high (50–55%) in HCC patients [16–19]. Recently, concerning resectable HCC, our group reported that FDG uptake evaluated by pre-operative PET is associated with tumour differentiation and post-operative survival in HCC patients treated with partial hepatectomy [20, 21]. However, there has been no report regarding the relationship between prognosis and FDG uptake evaluated by post-therapeutic PET after non-operative therapy in patients with unresectable HCC.

The purpose of this study is to investigate retrospectively the efficacy of FDG PET as an in vivo marker for tumour viability of HCC after non-operative therapy and as a prognostic predictor for post-treatment overall survival in patients with unresectable HCC.

Materials and methods

Study population

From May 2003 to April 2008, 465 cases with HCC were admitted to our unit in Kyoto University Hospital for the wish to receive a radical operation or non-operative therapy. By computed tomography (CT) scan, magnetic resonance imaging (MRI) and other imaging modalities, 320 cases were diagnosed to be candidates for a curative operation and underwent surgery. Another 23 cases were diagnosed as having far-advanced HCC and only received palliative treatment. The other 122 cases were diagnosed as having unresectable HCC and treated by non-operative therapy. Inclusion criteria in the present study were as follows: (1) diagnosed as unresectable HCC by CT scan and MRI in pre-therapeutic evaluation, (2) treated with non-operative therapy (TACE, TAI, RFA, PEIT or systemic chemotherapy) and completed a single course of a therapeutic regimen, (3) diagnosed by FDG PET within 1 month after the end of non-operative therapy and (4) clinical follow-up more than 6 months after non-operative therapy. Exclusion criteria were as follows: (1) patients who received FDG PET only before non-operative therapy and (2) patients who received FDG PET more than 1 month after the end of non-operative therapy.

Of 122 cases with unresectable HCC, 67 were included in the present study, where 67 consecutive post-therapeutic FDG PET studies were performed in 58 patients within 1 month after the end of non-operative therapy (ranging from 0 to 28 days, mean interval of days: 10.9±10.9 days). In 29 patients, pre-therapeutic FDG PET was also performed within 3 months before the start of the therapy. Nine patients received non-operative therapies two times, with an interval of more than 1 month between each therapy (ranging from 32 to 1,960 days, mean interval of days: 328.5 days). Therefore, the patient who received non-operative therapies twice was counted as two cases for diagnosis of lesion viability and counted as a single patient at the time of the last post-therapeutic PET for analysis of survival. Finally, in this retrospective analysis, 67 cases (55 men and 12 women, mean age: 59.3±12.6 years) were analysed for diagnosis of lesion viability and 58 patients (46 men and 12 women, mean age: 60.8±12.1 years) were analysed for prediction of survival.

Before admission to Kyoto University Hospital, each patient gave written informed consent to becoming a possible candidate for retrospective clinical research (except for gene-

related researches), as required by the Kyoto University Human Study Committee.

Patient characteristics

Patient characteristics of 67 cases are shown in Table 1. The chemotherapeutic agents used in TACE, TAI and systemic chemotherapy were as follows: fluorouracil (5-FU) and 5-FU with cisplatin (CDDP) for TACE; 5-FU with CDDP and 5-FU with interferon for TAI; 5-FU, Farmorubicin (Farm) and gemcitabine (GEM) for systemic chemotherapy. The clinical stage of HCC was analysed at first before the treatment based on the criteria of the International Union Against Cancer (UICC) using several imaging modalities (CT, MRI and/or angiography and/or PET if available) [22]. The clinical stage of HCC was re-analysed at the time of post-therapeutic PET based on UICC criteria using PET results and other imaging modalities. Analyses using Milan criteria for the selection of liver transplantation were evaluated before the treatment based on the size and the number of tumours determined from imaging modalities using CT or MRI (single tumour: 5 cm or less in size; or three or less tumours: each 3 cm or less in size; and no macrovascular invasion) [23]. Analyses using Milan criteria were also re-evaluated at the time of post-therapeutic PET based on imaging modalities including PET. Thirty-seven patients

Table 1 Patient characteristics of 67 cases (58 patients)

Characteristic	Value	Characteristic	Value
Age (years)		Past history of therapy[a], *n* (%)	
Mean±SD	59.3±12.6	Partial resection	33 (49)
Range	32–80	LDLT	2 (3)
Gender, *n* (%)		TACE	51 (76)
Male	55 (82)	TAI	38 (57)
Female	12 (18)	RFA	31 (46)
Tumour differentiation, *n* (%)		PEIT	12 (18)
Well	3 (4)	Child-Pugh classification at pre-treatment, *n* (%)	
Moderately	16 (24)	A	38 (57)
Poorly	20 (30)	B	29 (43)
Unknown	28 (42)	Child-Pugh classification at PET study, *n* (%)	
Target therapy in the present study, *n* (%)		A	38 (57)
TACE	23 (34)	B	26 (39)
TAI	30 (45)	C	3 (4)
RFA	5 (7)	Child-Pugh score at PET study	
TACE+PEIT	1 (1)	Mean±SD	6.4±1.4
TAI+RFA	1 (1)	Aetiology of hepatitis, *n* (%)	
Systemic chemotherapy	7 (10)	HBV	19 (28)
Clinical stage at pre-treatment, *n* (%)		HCV	40 (60)
UICC, 6th edition		HBV+HCV	4 (6)
Stage II–III	47 (70)	Alcoholic	2 (3)
Stage IV	20 (30)	Unknown	2 (3)
Milan criteria at pre-treatment, *n* (%)		Pathological evaluation of hepatic parenchyma	
Fulfilled	21 (31)	Grade of hepatitis, *n* (%)	
Beyond	46 (69)	None	2 (3)
Clinical stage at post-PET evaluation, *n* (%)		Low	22 (38)
UICC, 6th edition		Moderate	12 (21)
Stage II–III	39 (58)	High	1 (2)
Stage IV	28 (42)	Not available	30 (36)
Milan criteria at post-PET evaluation, *n* (%)		Grade of fibrosis, *n* (%)	
Fulfilled	18 (27)	None	3 (5)
Beyond	49 (73)	Low	9 (16)
		Moderate	7 (12)
		High	18 (31)
		Not available	30 (36)

UICC International Union Against Cancer, TNM classification, *PET* positron emission tomography, *TACE* transcatheter arterial chemoembolization therapy, *TAI* transcatheter arterial infusion chemotherapy, *RFA* radiofrequency ablation therapy, *PEIT* percutaneous ethanol injection therapy, *LDLT* living donar liver transplantation, *HBV* hepatitis B virus, *HCV* hepatitis C virus

[a] Including overlapping therapy

received pathological evaluation of lesions and surrounding liver parenchyma by biopsy at the time of RFA or PEIT (at the present therapy or at the previous one within 6 months before the present therapy, $n=27$) or by surgical resection (within 2 weeks after the post-therapeutic PET, $n=10$). Activity grades of hepatitis and fibrosis were also evaluated in surrounding liver parenchyma by well-experienced pathologists using four-grade scales.

Tumour markers, including serum alpha-fetoprotein (αFP), lens culinaris agglutinin-reactive fraction of serum αFP (αFP-L3 fraction) and protein induced by vitamin K absence or antagonist II (PIVKA-II), were evaluated before the non-operative therapy and at the time of post-therapeutic PET. The presence of positive results in all these three tumour markers (αFP=400 or more, αFP-L3=15 or more and PIVKA-II=400 or more) was defined as "triple plus".

PET study

^{18}F was produced by ^{18}O(p, n) ^{18}F reaction. ^{18}F-FDG was synthesized by the nucleophilic substitution method using an ^{18}F-FDG-synthesizing instrument F-100 (Sumitomo Heavy Industries, Co. Ltd., Tokyo, Japan) and a cyclotron, CYPRIS-325R (Sumitomo Heavy Industries, Co. Ltd., Tokyo, Japan). All patients were examined with a whole-body PET scanner with an 18-ring detector arrangement (Advance, General Electric Medical Systems, Milwaukee, WI, USA).

The patients fasted for more than 4 h before the injection of ^{18}F-FDG. All subjects received an intravenous injection of ^{18}F-FDG (296 ±74 MBq), and the acquisition of whole-body PET images started 50 min later. Data acquisition (emission and transmission scan) was performed in two-dimensional imaging mode with septae in place. Emission images were acquired for 3 min per bed position and each post-emission transmission scan was obtained for 1 min per position. Whole-body scanning (from head to upper thigh) was performed in each patient using five or six bed positions according to the height of each patient. The data were reconstructed using the ordered subsets expectation maximization method (OSEM) using 16 subsets, 3 iterations and 128×128 array size.

Image analysis

PET images were interpreted and analysed visually by two or three experienced nuclear medicine physicians (TH, YN, KI, TS) with all available clinical information. Next, these physicians had a discussion and made a final diagnosis. Diagnosis of lesion viability was performed separately in liver lesions and metastatic lesions with a two-category system, positive or negative. In the diagnosis of liver lesions, FDG uptake of a lesion was compared with background uptake of liver parenchyma. If a nodule showed remarkably higher uptake than the liver parenchyma, PET diagnosis was defined as positive. If a nodule showed similar or lower uptake than the surrounding liver parenchyma, PET diagnosis was defined as negative. In the diagnosis of metastatic lesions, FDG uptake of each lesion was compared with background uptake of surrounding normal tissue or with the contralateral normal tissue (when the lesion was located in the lung field). All PET diagnostic results were based on the diagnostic reports described in patient charts at the time of the clinical course, and the whole results were again confirmed by nuclear medicine physicians (TH, RN) with 100% concordance rate, retrospectively. When visual PET analysis was negative in the whole body and then known lesions or newly discovered metastatic lesions were confirmed as alive within 6 months after PET study, visual PET diagnosis on lesion viability was defined as false-negative. On the contrary, when visual PET analysis was positive in a lesion and the lesion was confirmed as necrotic or nonexistent within 6 months after PET study, visual PET diagnosis on lesion viability was defined as false-positive. For univariate and multivariate analysis of prognostic factors, a positive PET finding in any lesion in the body (hepatic or metastatic, known or unexpected) was defined as positive for the patient.

In addition, semi-quantitative analysis of ^{18}F-FDG uptake was also performed for univariate and multivariate analysis of prognostic factors. Regions of interest (ROIs) were defined on the target lesions in the transaxial tomograms of PET images by the PET-to-CT co-registration method using the automatic rigid/non-rigid body-deformable fusion software: Quantiva/BodyGuide (Tomographix IP Ltd., Toronto, Canada). The maximum standardized uptake value (SUV) was calculated for quantitative analysis of tumour ^{18}F-FDG uptake as follows:

$$\mathrm{SUV} = \frac{\mathrm{C(kBq/ml)}}{\mathrm{ID(kBq)/body\ weight\ (g)}}$$

where C represents tissue activity concentration measured by PET and ID represents the injected dose. The highest maximum SUV of the lesion in the whole body (hepatic or metastatic) was defined as the SUV of the patient.

Clinical confirmation

Lesion viability after treatment was confirmed by surgical resection in ten cases (surgery could be performed later because of the therapeutic effect of non-operative therapy) and by clinical follow-up at least more than 6 months in 57 cases. Overall survival was confirmed in patient records by clinical follow-up at least more than 6 months, in which patients received at least one of several imaging modalities as follow-up study every 3 months, including CT, MRI, angiography

and PET. The starting point and the end-point of survival were defined as the date of post-therapeutic PET study and the date of death, respectively. Overall cumulative survival rates were obtained using the Kaplan-Meier method.

Statistics

All values are expressed as mean±SD. All of the statistical analysis was performed using statistical software, JMP 4 J version (SAS Institute, Cary, NC, USA), in which p values <0.05 were considered statistically significant. Patients were stratified and analysed by univariate analysis using the log-rank test according to the following factors: age, gender, histological grade of tumour differentiation, type of non-operative target therapy in the present study, clinical stage at pre-treatment evaluation (UICC), Milan criteria at pre-treatment evaluation, clinical stage at post-PET evaluation (UICC), Milan criteria at post-PET evaluation, past history of therapy, Child-Pugh classification, aetiology of hepatitis, pathological grade of hepatitis, pathological grade of fibrosis as well as pre-therapeutic and post-therapeutic tumour markers, including serum αFP level, serum αFP-L3 fraction, PIVKA-II level and triple plus, and pre-therapeutic and post-therapeutic FDG PET-related factors [SUV and visual PET diagnosis (positive or negative)]. Cut-off values, such as αFP=400 ng/ml, αFP-L3=15%, PIVKA-II=400 AU/ml and SUV=5.0, were defined based on the previous reports [21, 24, 25]. According to the univariate analysis, eight significant factors [clinical stage at post-PET evaluation (UICC), Milan criteria at post-PET evaluation, Child-Pugh classification, pathological grade of hepatitis, αFP level, presence of triple plus, SUV and visual PET diagnosis] were selected for the multivariate analysis using the stratified Cox proportional hazards model. A comparison between high FDG and low FDG groups was analysed by Wilcoxon score or chi-square test for unpaired data. Survival curves were calculated by Kaplan-Meier analysis and the differences between high FDG and low FDG groups and the differences between L-L, L-H, H-L and H-H groups were compared using the log-rank test.

Results

Patient characteristics

Table 1 summarizes the patient characteristics. The average follow-up of living patients (n=35) was 483±413 days (range: 202–1,565 days), while the average follow-up of dead patients (n=23) was 253±162 days (range: 22–644 days). The clinical stage at pre-treatment was evaluated as stage II–III (n=47, 70%) vs stage IV (n=20, 30%) by UICC. However, the clinical stage at post-PET was stage II–III (n=39, 58%) vs stage IV (n=28, 42%) by UICC. This is because an unexpected distant metastasis was detected by post-therapeutic PET study in 13% of patients (n=9) and PET refuted the presence of a distant metastasis in 1% of patients (n=1). Similar results were observed in Milan criteria.

Diagnosis of lesion viability

Table 2 shows the results of clinical values of post-therapeutic FDG PET as the diagnosis of lesion viability and as the survival prediction in unresectable HCC patients.

As for visual diagnosis of lesion viability of post-therapeutic hepatic lesions, sensitivity was relatively low with the value of 62.8% (27/43 cases), while positive predictive value was high with the value of 96.4% (27/28 cases). Sixteen false-negative PET cases (37.2%) were confirmed as having residual liver tumours within 6 months by several procedures, such as surgical resection (n=5), biopsy at the time of follow-up RFA (n=1) and other imaging modalities (contrast-enhanced CT: n=6, angiography: n=3, MRI: n=1). In these cases, however, the course of disease progression was slow and controllable because these lesions tended to respond to the subsequent repeated therapies.

Table 2 Post-therapeutic FDG PET: visual diagnosis of lesion viability and survival prediction

	Viability of hepatic lesions (based on pathological evaluation and clinical follow-up of 6months)	Viability of metastasis (based on clinical follow-up of 6months)	Survival prediction[a] (death within 12months)	Survival prediction[b] (death within 24months)
Sensitivity	62.8% (27/43 cases)	78.6% (22/28 cases)	96.0% (24/25 cases)	92.5% (37/40 cases)
Specificity	95.8% (23/24 cases)	92.3% (36/39 cases)	68.0% (17/25 cases)	100% (7/7 cases)
Positive predictive Value	96.4% (27/28 cases)	88.0% (22/25 cases)	75.0% (24/32 cases)	100% (37/37 cases)
Negative predictive Value	59.0% (23/39 cases)	85.7% (36/42 cases)	94.4% (17/18 cases)	70.0% (7/10 cases)
Accuracy	74.6% (50/67 cases)	86.6% (58/67 cases)	82.0% (41/50 cases)	93.6% (44/47 cases)

[a] Excluding patients who are alive within 12 months

[b] Excluding patients who are alive within 24 months

As for the diagnosis of viability of metastatic lesions, the sensitivity (78.6%, 22/28 cases) was higher than that of hepatic lesions. The positive predictive value in metastatic lesions (88.0%, 22/25 cases) was lower than that in hepatic lesions (96.4%, 27/28 cases). Three false-positive cases for metastatic lesions were as follows: remnant stomach after distal gastrectomy mimicking peritoneal dissemination, sarcoid nodules mimicking mediastinal lymph nodes metastases and faint thoracic vertebral uptake mimicking bone metastasis. Ultimately, the visual diagnostic accuracy of post-therapeutic lesion viability was higher in the metastatic lesions (86.6%, 58/67 cases) than that in hepatic lesions (74.6%, 50/67 cases).

Survival prediction by FDG PET

Survival prediction by visual FDG PET in unresectable HCC patients treated by non-operative therapy is also summarized in Table 2. Of 18 patients diagnosed as negative by post-therapeutic PET, 17 survived more than 12 months (negative predictive value: 94.4%). All 37 patients diagnosed as positive by post-therapeutic PET died within 24 months (positive predictive value: 100%). Survival prediction in 24 months by FDG PET was quite accurate with the value of 93.6% (44/47 cases).

Univariate analysis of each prognostic factor

Table 3 shows the results of univariate analysis of each prognostic factor in 58 patients. Clinical stage (UICC) and Milan criteria at pre-treatment evaluation did not show significant prognostic value, while those at post-PET evaluation showed statistically significant prognostic values (p=0.001–0.0001). Pathological grade of hepatitis showed significance, while that of fibrosis did not. All of the pre-therapeutic tumour markers were not significant factors. As for the post-therapeutic tumour markers, αFP (=400 ng/ml) showed significance (p=0.001). Post-therapeutic triple plus was also significant in prognostic value (p=0.005), although only six patients were positive.

FDG PET as a prognostic factor

Table 3 also shows prognostic values of FDG PET analysis before and after the non-operative therapy. The factors "post-therapeutic visual PET diagnosis (positive or negative)" and "post-therapeutic SUV=5.0" showed significance (p=0.001). In contrast, pre-therapeutic FDG PET analysis did not show any significant value.

The results of multivariate analysis of prognostic factors for overall survival in unresectable HCC patients treated by non-operative therapy are shown in Table 4. The independent prognostic factor with highest statistical value was "post-therapeutic αFP (= 400 ng/ml)" (risk ratio=0.277, p=0.004), followed by post-therapeutic visual PET diagnosis (risk ratio=0.212, p=0.0056). On the other hand, the factor "SUV=5.0" was not significant as a predictor (risk ratio=0.889, p=0.810). "Clinical stage at post-PET evaluation (UICC stage IV)" and "Milan criteria at post-PET evaluation" also showed significant value (risk ratio=0.335 and 0.001, p=0.041 and 0.033, respectively). The other factors did not show any significance in the prediction of overall survival.

Based on the results of multivariate analysis, we classified the patients into two groups: high FDG group (diagnosed as positive at the post-therapeutic PET) and low FDG group (diagnosed as negative at the post-therapeutic PET). Figure 1a shows the survival curve of these two groups. The low FDG group showed higher survival (average survival: 607.9± 29.7 days) than the high FDG group (average survival: 327.5±40.1 days). The log-rank test showed a statistically significant difference in survival between these two groups (p<0.001). Table 5 reveals the characteristics of the two groups. Among the pre-treatment factors evaluated, UICC stage was the only significantly different one between the two groups. However, the other pre-treatment factors (age, gender, tumour differentiation, Milan criteria, target non-operative therapy, past history of therapy and pathological grade of hepatitis) were not different between the two groups. The other factors (clinical stages and Milan criteria at post-PET evaluation) showed significant differences between the two groups, but these differences were based on the PET results, where an unexpected distant metastasis was detected by post-therapeutic PET study in 13% of patients (n=9) and PET refuted the presence of a distant metastasis in 1% of patients (n=1). Therefore, clinical stages and Milan criteria at post-PET evaluation turned out to be different between the two groups as a result of FDG PET study. Pre-therapeutic tumour markers were not different in both groups. Post-therapeutic tumour markers were lower in the low FDG group because of the response to the target non-operative therapy. Although there was a significant difference in the factors of post-therapeutic FDG PET, there was no difference in the factors of pre-therapeutic PET (SUV and diagnosis). Thus, it may be said that there was no significant bias between the two groups before the target treatment.

Analysis using FDG uptake pattern

In the present study, 29 patients received pre-therapeutic FDG PET studies. According to pre- and post-therapeutic PET results, we classified these patients (n=29) into four groups by the pattern of FDG uptake as follows (Fig. 1b): low-low uptake group (L-L group) which consisted of patients who were diagnosed as negative in pre- and post-therapeutic PET studies (n=3); high-high uptake group (H-H group) which

Table 3 Univariate analysis of prognostic factors for overall survival in 58 patients

		Mean survival				Mean survival	
	n	days	*p*		*n*	days	*p*
Age (years)				Grade of fibrosis			
<60	26	438	0.76	None	3	158	0.77
≥60	32	465		Low	9	518	
Gender				Moderate	7	283	
Male	48	450	0.62	High	18	308	
Female	10	327					
Tumour differentiation							
Well	3	22	0.88	Pre-therapeutic tumour markers			
Moderately	16	487		αFP (ng/ml)			
Poorly	14	310		<400	34	489	0.12
Unknown	25	462		400 or higher	20	286	
Target therapy in the present study				αFP-L3 fraction (%)			
TACE[a]	22	498	0.13	<15	11	305	0.18
TAI[b]	26	318		15 or higher	18	287	
RFA	4	133		PIVKA-II (AU/ml)			
Systemic chemotherapy	6	339		<400	35	433	0.65
Clinical stage at pre-treatment				400 or higher	16	301	
UICC, 6th edition				Triple plus (αFP=400 or higher & αFP-L3=15 or higher & PIVKA-II=400 or higher)			
Stage II–III	42	475	0.30	Triple plus	6	317	0.76
Stage IV	16	276		Negative	44	421	
Milan criteria at pre-treatment							
Fulfilled	20	495	0.25				
Beyond	38	431		Post-therapeutic tumour markers			
Clinical stage at post-PET evaluation				αFP (ng/ml)			
UICC, 6th edition				<400	39	516	0.001[c]
Stage II–III	36	532	0.001[c]	400 or higher	19	262	
Stage IV	22	259		αFP-L3 fraction (%)			
Milan criteria at post-PET evaluation				<15	32	488	0.16
Fulfilled	17	all alive	0.0001[c]	15 or higher	23	302	
Beyond	41	376		PIVKA-II (AU/ml)			
Past history of therapy				<400	37	481	0.11
Partial resection ±	29/29	398/502	0.13	400 or higher	17	389	
LDLT ±	1/57	-		Triple plus (αFP=400 or higher & αFP-L3=15 or higher & PIVKA-II=400 or higher)			
TACE ±	43/15	458/290	0.90	Triple plus	6	218	0.005[c]
TAI ±	31/27	445/452	0.98	Negative	46	474	
RFA ±	28/30	317/471	0.88	Pre-therapeutic FDG PET			
PEIT ±	12/46	167/457	0.84	Visual PET diagnosis			
Child-Pugh classification at PET study				Positive	18	294	0.78
A	33	438	0.0001[c]	Negative	11	399	
B	22	322		SUV			
C	3	84		<5.0	15	419	0.73
Aetiology of hepatitis				5.0 or higher	13	278	
HBV	15	421	0.14	Post-therapeutic FDG PET			
HCV	37	490		Visual PET diagnosis			
Others	6	142		Positive	32	327	0.0001[c]
Pathological grade of hepatitis				Negative	26	608	
None	2	-	0.01[c]	SUV			
Low	22	487		<5.0	40	523	0.0001[c]
Moderate	12	268		5.0 or higher	18	227	
High	1	131					

αFP alpha-fetoprotein, *αFP-L3* lens culinaris agglutinin-reactive fraction of αFP, *PIVKA-II* protein induced by vitamin K absence or antagonist II, *FDG* fluorodeoxyglucose, *SUV* standardized uptake value

[a] Including PEIT

[b] Including overlapping therapy

[c] Significant by log-rank test

Table 4 Multivariate analysis of prognostic factors for overall survival

Prognostic factors	Risk ratio	(95% confidence interval)	*p*
Clinical stage at post-PET evaluation			
UICC, 6th edition, stage IV	0.335	(0.094–0.959)	0.041[a]
Milan criteria at post-PET evaluation			
Fulfilled	0.001	(–0.891)	0.033[a]
Child-Pugh classification at PET study			
B or C	0.482	(0.136–0.482)	0.218
Pathological grade of hepatitis			
Moderate or high	1.155	(0.159–9.122)	0.887
Post-therapeutic tumour markers			
αFP (ng/ml)=400	0.277	(0.089–0.680)	0.004[a]
Triple plus (αFP=400 & αFP-L3=15 & PIVKA-II=400)	3.964	(0.869–25.039)	0.077
Post-therapeutic FDG PET			
Visual PET diagnosis: positive	0.212	(0.042–0.661)	0.0056[a]
SUV=5	0.889	(0.337–2.451)	0.810

[a] Significant in Cox proportional hazards model

consisted of patients who were diagnosed as positive in pre- and post-therapeutic PET studies (n=10); low-high group (L-H group) which consisted of patients who were diagnosed as negative before the treatment and then showed positive uptake in the post-therapeutic PET study (n=8) (Fig. 2); and high-low group (H-L group) which consisted of patients who were diagnosed as positive before the treatment and then showed negative uptake in the post-therapeutic PET study (n=8) (Fig. 3). Figure 1b shows the survival curve of these four groups. The H-L group showed the highest survival rate in these four groups and all of them (n=8) still survived in the follow-up period. The H-H group showed the lowest survival curve. There was no difference in survival between the L-L group and L-H group. The log-rank test showed a significant different between these groups.

Discussion

FDG PET is considered as a well-established non-invasive diagnostic tool for the detection of malignant tumours [26, 27], staging and monitoring of chemotherapeutic response [28, 29] in several cancers. Shiomi et al. reported that FDG PET is useful not only for the evaluation of the malignancy but also for the prediction of outcome in patients with HCC [15]. For HCC, however, several investigators have reported that the sensitivity of FDG PET is low in the detection of HCC [17–19]. Relatively low FDG accumulation in HCC can be explained by the activity of enzymes involved in glucose metabolism. The activity of glucose-6-phosphatase (G-6-Pase), which converts FDG-6-P to FDG, is reported to be high in normal liver and nearly zero in the vast majority of tumours, including metastatic liver tumours [14, 30]. In contrast, the enzyme activity has been reported to vary widely in individual HCC; well-differentiated HCC cells exhibit an FDG metabolism similar to that of normal liver tissue, whereas undifferentiated HCC cells do not [21]. Therefore, well-differentiated HCC tends to accumulate similar amounts of FDG as normal liver, which results in relatively lower SUV. However, this enzymatic theory for FDG uptake can only be applicable in pre-operative, non-treated HCCs. As an imaging modality for the early evaluation of treatment response after non-operative therapy for HCC, the role of FDG PET has not been established, nor reported so far.

Interventional therapy, such as TACE or TAI, is considered to be an effective palliative treatment in patients with HCC [31, 32]. However, a meta-analysis of randomized clinical trials showed that a survival advantage associated with therapeutic chemoembolization versus supportive care alone has not been clearly proven so far [33]. Therefore, it is clinically important to analyse the therapeutic effect of non-operative therapy as soon as possible, because inefficacious palliative treatment may be not only useless but also harmful for patients with advanced HCC. Conventional imaging modalities, such as CT or MRI, cannot satisfy clinicians in that context, because therapy evaluation by these anatomical imaging modalities requires sufficient time to confirm tumour shrinkage [34, 35]. Herein, PET, as a metabolic imaging modality, is expected to be useful in electing to proceed or terminate therapy. Our data in the present study showed that FDG PET could evaluate therapeutic effect and prognostic value in patients with unresectable HCC. To our knowledge, the present study is the first report evaluating the effectiveness of FDG PET in the early therapeutic response evaluation in unresectable HCC patients treated by non-operative therapies.

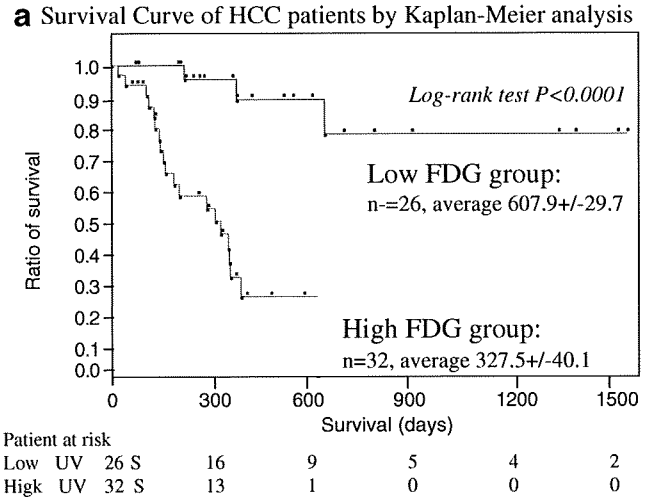

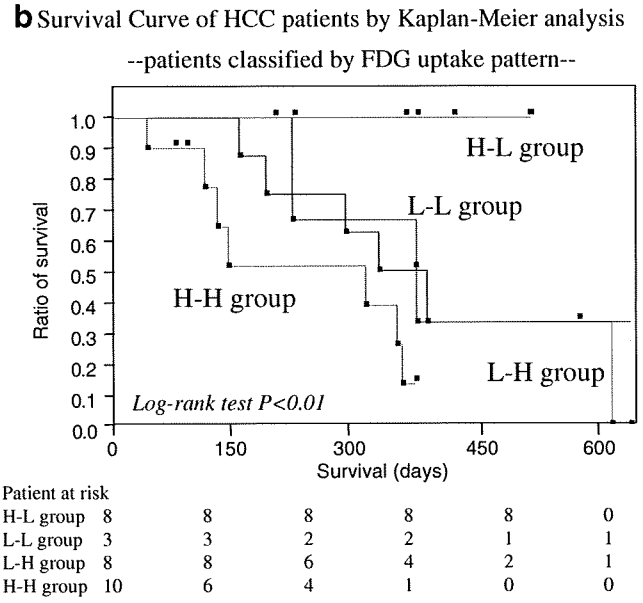

Fig. 1 Survival curve of HCC patients by Kaplan-Meier analysis. **a** The overall survival rate in HCC patients treated by non-operative therapy was significantly higher in the low FDG group than that in the high FDG group ($p<0.0001$). **b** The overall survival rate in four groups of patients classified by the FDG uptake pattern (see exact definition in the text) is shown. The H-H group showed poor survival. On the other hand, the H-L group showed the best survival with 100% survival rate in the follow-up period. There was no difference between the L-H group and L-L group. The log-rank test showed that there was a significant difference between the four groups ($p<0.01$)

Our principal finding is that visual FDG PET diagnosis after non-operative therapy is an independent predictor of survival in unresectable HCC patients. This is compatible with a variety of previous studies performed in other malignancies [36–38]. Table 2 also clearly reveals the advantage of FDG PET diagnosis in early post-therapeutic evaluation with respect to the prediction of patient survival. High negative predictive value (94.4%) means that patients with negative post-therapeutic PET result are supposed to survive at least 12 months, while high positive predictive value (100%) means that patients with positive post-therapeutic PET result are supposed to die within 24 months. We believe that post-therapeutic FDG PET after non-operative therapy would make a great contribution in the clinical management of patients with unresectable HCCs, such as in electing to proceed or terminate therapy, altering the chemotherapeutic regimen, choosing treatment modalities or in other decisions.

On the other hand, FDG PET within 1 month after non-operative therapy is not sensitive in the diagnosis of lesion viability. Table 2 shows the limitation of FDG PET diagnosis in early post-therapeutic evaluation of HCC. Relatively low sensitivity (62.8%) and low negative predictive value (59%) in the analysis of viability of hepatic lesions suggest that negative FDG PET findings cannot ensure the complete remission of HCC after therapy. At the current moment, it is not clear what the cellular or tissue condition of the tumour is when FDG PET is negative after the non-operative therapy. It is implied, however, that they lie dormant with temporary enzymatic or other dysfunction, but can survive.

Our result shown in Fig. 2 suggests that even if FDG uptake shows a partial reduction after non-operative treatment, as observed in the H-H group, HCCs with constant positive PET finding tend to have more aggressive malignant potential. Long survival may not be expected, and continued treatment or a newly introduced therapeutic procedure would be required. On the contrary, the result of the H-L group suggests that prognostic improvement can be expected when FDG uptake disappeared. These observations provide helpful information for the management of patients with unresectable HCCs.

Bibliographically, a number of reports have been published as for the prognostic factors in patients with HCC treated by surgical procedures. Imamura et al. showed that non-anatomical resection, presence of microscopic vascular invasion and serum αFP were significant risk factors contributing to early recurrence of HCC after hepatectomy [10]. Miyaaki et al. also showed that αFP-L3 and PIVKA-II levels are potential indicators of a poor prognosis in surgically resected HCC [39]. For patients treated with liver transplantation, presence of capsule, αFP levels and viral cirrhosis were independent factors for survival [40]. Above all, the Milan criteria (single tumour: 5 cm or less in size; or three or less tumours: each 3 cm or less in size; and no macrovascular invasion) are known for their excellent outcome in the prediction of survival in patients treated with liver transplantation [24]. All these data in patients treated by surgical procedures seem to be consistent with our results. In the present study, multivariate analysis revealed that the post-therapeutic tumor marker αFP, clinical staging and Milan criteria at post-PET and visual PET diagnosis are significant prognostic factors (Table 4). This is also basically compatible (except for PET diagnosis) with the previous report using multivariate analysis

Table 5 Comparison of high FDG and low FDG groups

	High FDG group (n=32)	Low FDG group (n=26)	p
Age (years)			
Mean±SD	59.5±13.3	62.4±10.4	n.s.
Range	34–80	42–78	
Gender, n (%)			
Male	26 (81)	20 (77)	n.s.
Female	6 (19)	6 (23)	
Tumour differentiation, n (%)			
Well	2 (6)	1 (4)	n.s.
Moderately	10 (31)	6 (23)	
Poorly	8 (25)	6 (23)	
Unknown	12 (38)	13 (50)	
Target therapy in the present study, n (%)			
TACE	9 (28)	12 (46)	n.s.
TAI[a]	17 (53)	9 (35)	
RFA	1 (3)	3 (12)	
TACE+PEIT	0 (0)	1 (4)	
Systemic chemotherapy	5 (16)	1 (4)	
Clinical stage at pre-treatment, n (%)			
UICC, 6th edition			
Stage II–III	19 (59)	23 (88)	0.01[c]
Stage IV	13 (41)	3 (12)	
Milan criteria at pre-treatment, n (%)			
Fulfilled	10 (31)	10 (38)	n.s.
Beyond	22 (69)	16 (62)	
Clinical stage at post-PET evaluation, n (%)			
UICC, 6th edition			
Stage II–III	13 (41)	23 (88)	0.0001[c]
Stage IV	19 (59)	3 (12)	
Milan criteria at post-PET evaluation, n (%)			
Fulfilled	4 (13)	13 (50)	0.002[c]
Beyond	28 (88)	13 (50)	
Past history of therapy[a], n (%)			
Partial resection	17 (53)	12 (46)	n.s.
LDLT	1 (3)	0 (0)	
TACE	24 (75)	19 (73)	
TAI	17 (53)	14 (54)	
RFA	16 (50)	12 (46)	
PEIT	5 (16)	7 (27)	
Child-Pugh classification at PET study, n (%)			
A	21 (66)	12 (46)	0.02[c]
B	8 (25)	14 (54)	
C	3 (9)	0 (0)	
Child-Pugh score at PET study			
Mean±SD	6.3±1.6	6.6±1.1	n.s.
Pathological grade of hepatitis			
None or low	14 (44)	10 (38)	n.s.
Moderate or high	8 (25)	5 (19)	
	(n=22)	(n=15)	
Pre-therapeutic tumour markers			
αFP (ng/ml)	12,926±37,934	6,734±30,440	n.s.
αFP-L3 fraction (%)	37.2±29.9	42.6±33.8	n.s.
PIVKA-II (AU/ml)	8,666±25,900	10,093±43,296	n.s.
	(n=32)	(n=23)	
Post-therapeutic tumour markers			
αFP (ng/ml)	14,532±35,462	306±796	0.001[b]
αFP-L3 fraction (%)	38.5±28.6	35.1±31.9	n.s.
PIVKA-II (AU/ml)	9,206±34,433	531±1,938	0.005[b]
Pre-therapeutic FDG PET			
SUV	4.9±2.5	5.8±3.6	n.s.
Diagnosis: positive vs negative	10 vs 8	8 vs 3	n.s.
	(n=18)	(n=11)	
Post-therapeutic FDG PET			
SUV	7.0±4.6	2.6±0.9	0.0001[b]

[a] Including overlapping therapy

[b] Significant by Wilcoxon score

[c] Significant by chi-square

in TACE patients, in which αFP level, unilobar tumours and/or Child-Pugh score are the prognostic factors in HCC patients treated with TACE [41, 42]. Based on the evidence reported, it seems reasonable to suppose that our results in prognostic factor analysis have considerable validity. Although αFP level was the strongest, the most convenient and the less expensive prognostic factor in the present study, FDG PET has an advantage in the detection of active lesions. In addition, PET results would be helpful when the post-therapeutic αFP response was controversial. For example, in Fig. 3 post-therapeutic αFP showed a rise while PET diagnosis showed negative result. Thus, we believe that FDG PET has important clinical value in the prognostic prediction and in the decision-making process of patient management. It is to be noted that clinical staging and Milan criteria at post-PET were significant prognostic factors, while those at pre-treatment were not. It again emphasizes the importance of FDG PET diagnosis, not only for the prognostic value of its own, but also in the sense of detection of unknown metastases and the resultant renewed clinical

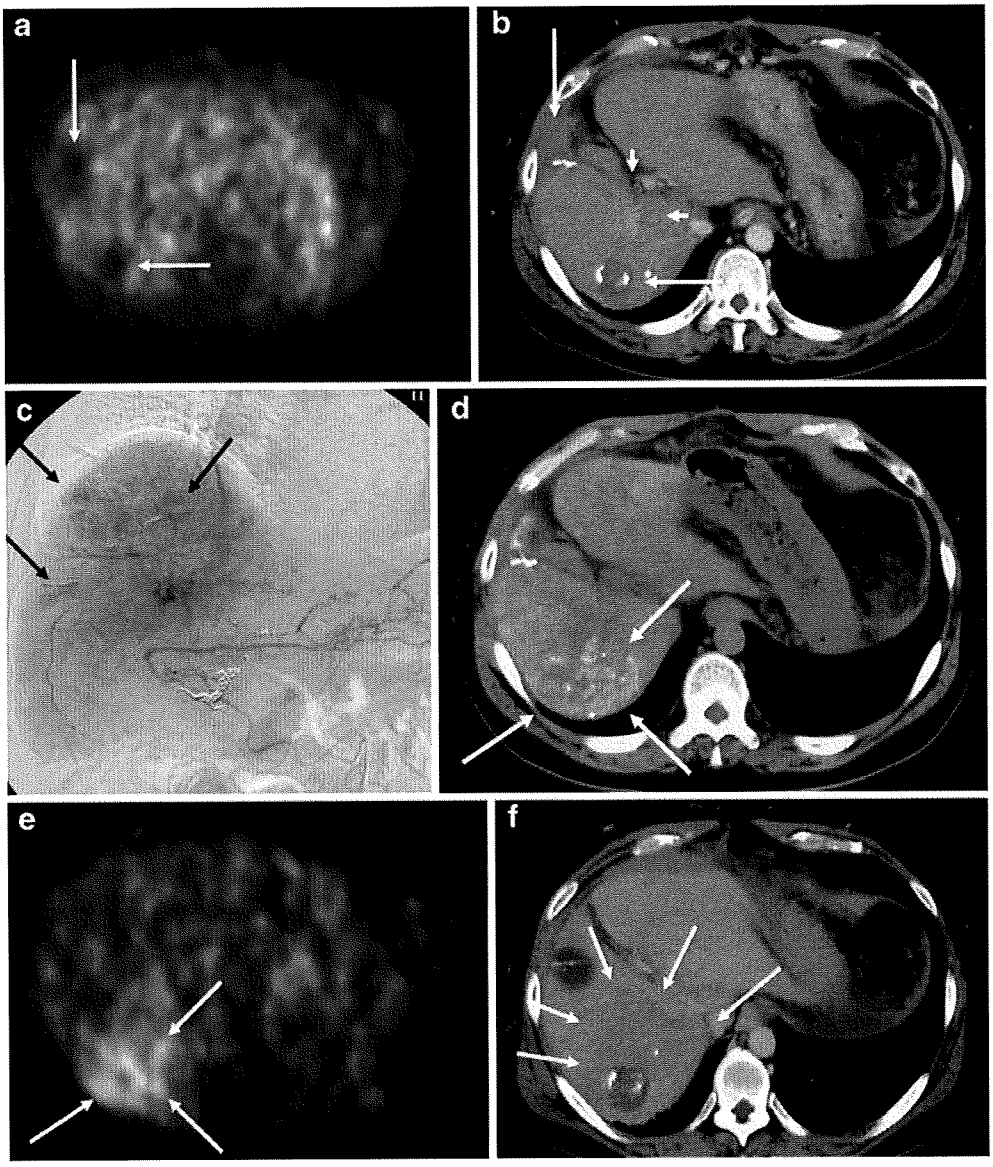

Fig. 2 A case of the L-H group: a 50-year-old man with unresectable moderately differentiated HCC, based on hepatitis type C. Past history: HCC was detected 2 years ago, and partial hepatectomy (S5) with splenectomy, TACE and RFA had been already performed. Present history: multiple recurrent nodules in bilateral lobes were detected with increased tumour markers. Then, an arterial catheter was inserted in the proper hepatic artery and TAI using biweekly infusion of CDDP and 5-FU had been performed via an indwelling arterial port. However, the arterial port was decannulated 80 days before the target TAI therapy because of the complication in the local subcutaneous tissue. **a** FDG PET was performed at 73 days before the TAI therapy. Defects of FDG uptake (*arrows*) were observed in the right lobe of the liver; therefore, visual PET diagnosis was negative at this time (SUV: 3.76 in the right posterior section). Tumour markers at this time were as follows: αFP: 632 ng/ml, αFP-L3: 53.4%, PIVKA-II: 193. **b** Follow-up contrast-enhanced CT scan was performed at 23 days before the TAI therapy. Faint enhancement at arterial phase was observed in the right posterior section (*arrowheads*) and lateral lobe (not shown). Therefore, the TAI therapy was scheduled because of these multiple nodules. Low-density areas corresponding to the defects in PET are also shown (*arrows*). **c** Angiography at the time of the non-operative therapy. Vague and faint multiple tumour stains were observed in the whole liver (*arrows*). Arterial infusion chemotherapy using one shot of water-soluble CDDP (50 mg) and lipiodol (5CC) was performed via the proper hepatic artery. **d** Follow-up plain CT scan was performed at 7 days after the TAI therapy. Scattered lipiodol deposition was observed in the right posterior section (*arrows*), which corresponded to the tumour stain at angiography. **e** FDG PET was performed at 14 days after the TAI therapy. Increased FDG uptake was observed in the right posterior section corresponding to the lipiodol deposition (SUV: 5.99) (*arrows*). Tumour markers showed a rise despite the therapy: αFP: 1860 ng/ml; αFP-L3: 46.4%; PIVKA-II: 1670. **f** Follow-up contrast-enhanced CT scan was performed at 35 days after the TAI therapy. Widespread low enhancement in the right posterior section at portal phase was clearly revealed at this CT scan (*arrows*). Since then, the recurrent HCC showed a rapid increase with portal vein tumor thrombus, and this patient died 187 days after the TAI therapy because of liver failure